An evaluation of MPM, GIMP and CMPM in geotechnical problems considering large deformations

Gonzalez Acosta, Leon; Vardon, Phil; Hicks, Michael

Publication date
2017

Document Version
Accepted author manuscript

Published in
Proceedings of the 15th International Conference of the International Association for Computer Methods and Advances in Geomechanics

Citation (APA)
Gonzalez Acosta, L., Vardon, P., & Hicks, M. (2017). An evaluation of MPM, GIMP and CMPM in geotechnical problems considering large deformations. In *Proceedings of the 15th International Conference of the International Association for Computer Methods and Advances in Geomechanics : 19-23 October 2017, Wuhan, China*

Important note
To cite this publication, please use the final published version (if applicable).
Please check the document version above.

An evaluation of MPM, GIMP and CMPM in geotechnical problems considering large deformations

L. Gonzalez Acosta[a]*, P.J. Vardon[a] and M.A. Hicks[a]
[a] *Geo-Engineering Section, Delft University of Technology, the Netherlands*
* J.L.GonzalezAcosta-1@tudelft.nl

Abstract

Stress oscillations are a common phenomenon in the material point method (MPM), since this numerical method typically uses regular finite element (FE) shape functions to map variables from surrounding nodes to material points and vice versa, independently of the locations of the material points within an element. In integration this leads to a quadrature rule error and, in strain and stress calculations, derivatives of typical FE shape functions are discontinuous across element boundaries and do not give accurate results away from Gauss point locations within elements. In geotechnical analysis, the constitutive behaviour is generally stress-dependent, and therefore stress oscillations can cause severe inaccuracies in the calculated mechanical behaviour, including the development of wrong elasto-plastic quantities. Several attempts to improve stress recovery and reduce quadrature errors have been developed, but seldom has a full comparison between methods been made. In this paper, benchmark small scale and slope stability problems have been examined in order to compare the relative performance of the classic material point method (MPM), the generalized interpolation material point (GIMP) method and the new compound material point method (CMPM).

Keywords: CMPM, GIMP, Material Point Method, Slope Stability, Softening, Stress Oscillation.

1. Introduction

The material point method (MPM) [1-2] has proven to be a valid numerical technique to simulate geotechnical behaviour, especially when simple constitutive models are used, since these models are related with variables less sensitive to stress oscillations, as in the case of the Von Mises criterion. In reality, the use of complex constitutive models is often needed to ensure the correct evolution of the mechanical behavior of the soil, and therefore the issue of stress oscillations should be addressed.

The generalized interpolation material point (GIMP) method [3] was created to overcome errors caused by the use of regular finite element (FE) shape functions in MPM. In this method, FE shape functions are replaced by C^1 shape functions, ensuring continuity in stresses when material points cross inter-element boundaries. As well as GIMP, the compound material point method (CMPM) [4] was developed to reduce the fluctuation in stresses caused by the ill-posed material point locations. CMPM uses C^n shape functions, and the evaluation of strains at each material point comes from the interpolation of displacements from all nodes of the element in question and the neighbouring elements, instead of using only nodes inside a support domain as in GIMP.

In the first section of this paper, the theory of MPM, GIMP and CMPM are outlined, followed by the analysis of a benchmark problem to demonstrate how stresses oscillate using these techniques. A vertical cutting problem is then analyzed, to visualise how each method predicts the stresses developed during slope failure.

2. Theoretical formulation

Since MPM shares similarities with the FEM continuum mechanics framework [5-6], the weak form of momentum conservation is, as typical in FEM, given as

$$\int_{\Omega} \rho \mathbf{a} \cdot \delta u dV + \int_{\Omega} \rho \boldsymbol{\sigma} \nabla \delta u dV = \int_{\Omega} \rho \mathbf{b} \cdot \delta u dV + \int_{\Gamma} \rho \boldsymbol{\tau}^{s} \delta u dA \tag{1}$$

where ρ is the material density, $\mathbf{a}$ is the acceleration, δu is the virtual displacement, V is the body volume, $\boldsymbol{\sigma}$ is the Cauchy stress, $\mathbf{b}$ are the body forces, $\boldsymbol{\tau}^{s}$ are the prescribed tractions, Γ is the traction boundary, and Ω is the solution domain. Since the domain is represented as points of mass, the total mass in the domain can be computed as [7]

$$\sum_{p=1}^{n_p} m_p = \int_{\Omega} \rho(\mathbf{x}) dV \tag{2}$$

where m_p is the mass of the point p, n_p is the number of points in the domain, and $\mathbf{x}$ is the position of any point. Substituting Eq. (2) into Eq. (1) gives

$$\sum_{p=1}^{n_p} m_p \delta u(\mathbf{x}_p)\mathbf{a}(\mathbf{x}_p) + \sum_{p=1}^{n_p} m_p \boldsymbol{\sigma}(\mathbf{x}_p)\nabla \delta u(\mathbf{x}_p) = \sum_{p=1}^{n_p} m_p \mathbf{b}(\mathbf{x}_p)\delta u(\mathbf{x}_p) + \sum_{p=1}^{n_p} m_p \boldsymbol{\tau}^{\$}(\mathbf{x}_p)\delta u(\mathbf{x}_p) \tag{3}$$

Using the Galerkin method, the virtual displacement is approximated as

$$\delta u(\mathbf{x}_p) = \sum_{v=1}^{n_n} \delta u_v N_v(\mathbf{x}_p) \tag{4}$$

where N_v is the shape function, subscript v denotes grid node v, n_n is the number of nodes in the element, and $\mathbf{x}_p$ is the material point position in the element. Substituting Eq. (4) into Eq. (3) and following standard FE procedures [8], leads to

$$\sum_{p=1}^{n_p} m_p \left(N_v(\mathbf{x}_p)\mathbf{a}_p\right) + \sum_{p=1}^{n_p} m_p \boldsymbol{\sigma}(\mathbf{x}_p)\nabla N_v(\mathbf{x}_p) = \sum_{p=1}^{n_p} m_p \mathbf{b}(\mathbf{x}_p) N_v(\mathbf{x}_p) + \sum_{p=1}^{n_p} m_p \boldsymbol{\tau}^{\$}(\mathbf{x}_p) N_v(\mathbf{x}_p) \tag{5}$$

It is evident that conservation of momentum is achieved by using shape functions (terms 1, 3 and 4 in Eq. (5)) and shape functions derivatives (term 2 in Eq. (5)). This leads to a variational inconsistency, which becomes more important during material point element crossing, due to term 2 being discontinuous between elements when using C^0 shape functions. In general, MPM is limited to linear (C^0) shape functions, since the use of quadratic elements can lead to errors when negative parts of the shape functions are used, in particular in the mass matrix. In addition, for implicit formulations, during the calculation of the stiffness matrix the non-Gaussian position of the material point in the numerical integration can cause some terms of the strain-displacement matrix to become negative, leading to an unrealistic element deformation.

It has been proposed to reduce the imbalance caused by the use of C^0 shape functions by using modified linear shape functions, so that they become C^1 shape functions, improving the spatial integration [9-10]. This approach is used in GIMP, where the original FE shape functions and their gradients are replaced by a set of continuous shape functions and shape function gradients with a nonlocal support, diminishing the imbalance cause by local FE shape functions and eliminating element crossing noise. If a regular grid is used, considering 2 points per element for the initial condition and avoiding distortion of the material point domain, GIMP shape functions can be computed, for example for 1D elements, as [11]

$$N_i(\xi) = \begin{cases} (7 - 16\xi^2)/8 & |\xi| \le 0.25 \\ 1 - \xi & 0.25 \le |\xi| \le 0.75 \\ (5 - 4\xi)^2/16 & 0.75 \le |\xi| \le 1.25 \\ 0 & |\xi| \ge 1.25 \end{cases} \tag{6}$$

where ξ is the local coordinate. Fig. 1 shows the GIMP shape function given by Eq. (6).

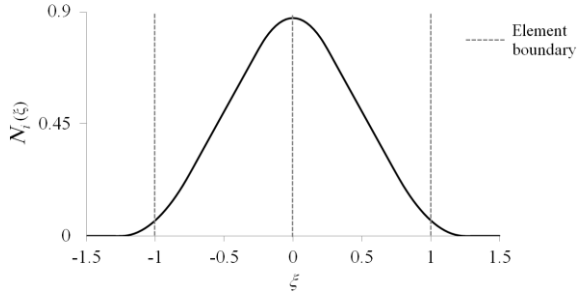

Fig. 1. GIMP shape function support domain.

CMPM uses C^n shape functions to calculate the strains and stresses, by increasing the solution domain using nodes from the current and neighbouring elements, leading to a smooth distribution within an element. CMPM does not eliminate element crossing noise, but it reduces oscillations caused by discontinuous stresses and lower order shape function derivatives, leading to a smaller stress discontinuity between elements. Fig. 2 shows two possible positions for a material point (labeled *mp*) in the domain; in a boundary element and in a centre element. To interpolate strains in a 1D element, the boundary and centre shape functions (N_i^b and N_i^c respectively) are computed as [12]

$$\begin{bmatrix} N_1^b \\ N_2^b \\ N_3^b \end{bmatrix} = \begin{bmatrix} \frac{1}{8}(\xi-1)(\xi-3) \\ \frac{-1}{4}(\xi+1)(\xi-3) \\ \frac{1}{8}(\xi+1)(\xi-1) \end{bmatrix} \tag{7}$$

$$\begin{bmatrix} N_1^c \\ N_2^c \\ N_3^c \\ N_4^c \end{bmatrix} = \frac{1}{16}\begin{bmatrix} \frac{-1}{3}(\xi^3-3\xi^2-\xi+3) \\ (\xi^3-\xi^2-9\xi+9) \\ -(\xi^3+\xi^2-9\xi-9) \\ \frac{1}{3}(\xi^3+3\xi^2-\xi-3) \end{bmatrix} \tag{8}$$

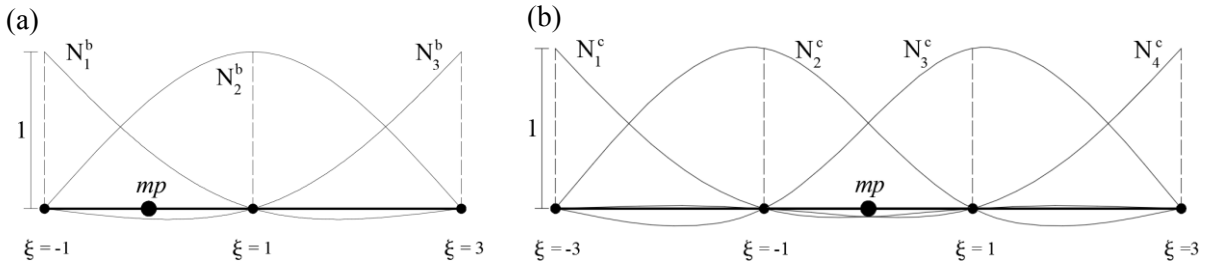

Fig. 2. Shape functions for (a) a boundary element, and (b) a centre element.

It is important to emphasise that CMPM shape functions are only used to evaluate strains, and that regular FE shape functions are still used to compute the governing equation matrices.

In the following sections, implicit and an explicit codes are used to solve benchmark and slope stability problems (respectively). Note that stress oscillations caused by quadrature errors and shape function discontinuities occur in both these methods (implicit and explicit), but in the implicit method extra oscillations are observed due to the stiffness matrix integration.

3. Stress oscillation in MPM, GIMP and CMPM

An illustration of stress oscillations using MPM, GIMP and CMPM is presented in this section. An axisymmetric analysis of a thick-walled hollow cylinder has been carried out using 4 noded quadrilateral elements. Radial displacement is applied incrementally at the inner boundary ($r = r_i$) and the outer boundary is completely fixed ($r = r_e$), as shown in Fig. 3. The cylinder is assumed to be linear elastic, with E = 25000 kPa and ν = 0.3. The solution is obtained using a quasi-static implicit code.

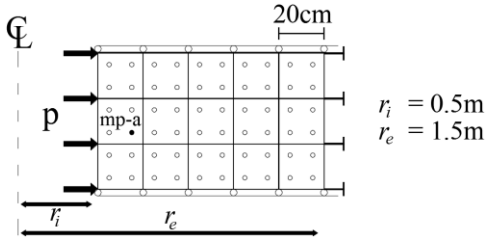

Fig. 3. Thick-walled cylinder under internal pressure.

Differences between MPM, GIMP and CMPM stress oscillations are shown in Fig. 4, in which a displacement of 1.5 cm has been applied in a single step and the stress computed across the domain.

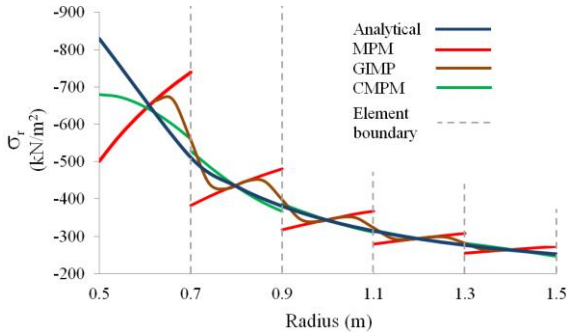

Fig. 4. Radial stress oscillation using MPM, GIMP and CMPM.

Fig. 4 shows that radial stresses computed using GIMP and CMPM are closer to the analytical solution, whereas MPM stresses oscillate more. It is also evident that the CMPM solution oscillates significantly less than that for GIMP, although the GIMP solution is continuous across element boundaries. However, the GIMP solution is incomplete at the domain boundaries, since interpolation using ghost nodes was not implemented in this example. Since an implicit code is used, stiffness matrices are used to solve the equation of motion. Following a similar approach as in FEM, the stiffness matrix is computed as

$$\mathbf{K}_m = \sum_{p=1}^{S_p} \left(\mathbf{B}^{\mathrm{T}}\mathbf{D}\mathbf{B}\right) W_p V_p \tag{9}$$

where S_p is the number of material points within an element, **B** is the strain-displacement matrix, **D** is the elastic stress-strain matrix, W_p are the material point integration weightings, initially selected to have a value of 1, and V_p are the material point volumes. As can be seen in Eq. (9), the element stiffness matrix is a function of the number of material points inside an element, leading to a variation of the element stiffness during element crossing and thereby to the oscillation of stresses. An alternative weighting value is here proposed to be a function of both the element volume and the volume of the material points within the element:

$$W_p = \frac{V}{\sum_{p=1}^{e_p} V_p} \tag{10}$$

where V is the element volume and e_p is the number of material points in the element. In Fig. 5, the deviatoric stress (q) of a single material point (**mp-a** from Fig. 3) is plotted for 50 steps, each of 1.5 cm. As can be seen in Fig. 5a, stress oscillation is observed using all methods, but GIMP and CMPM follow the analytical solution more closely. It is also noticeable that, during element crossing, a jump in the stresses occurs. The effect of using the modified weighting value is shown in Fig. 5b. The results inprove considerably, due to stiffness in the domain being more evenly distributed.

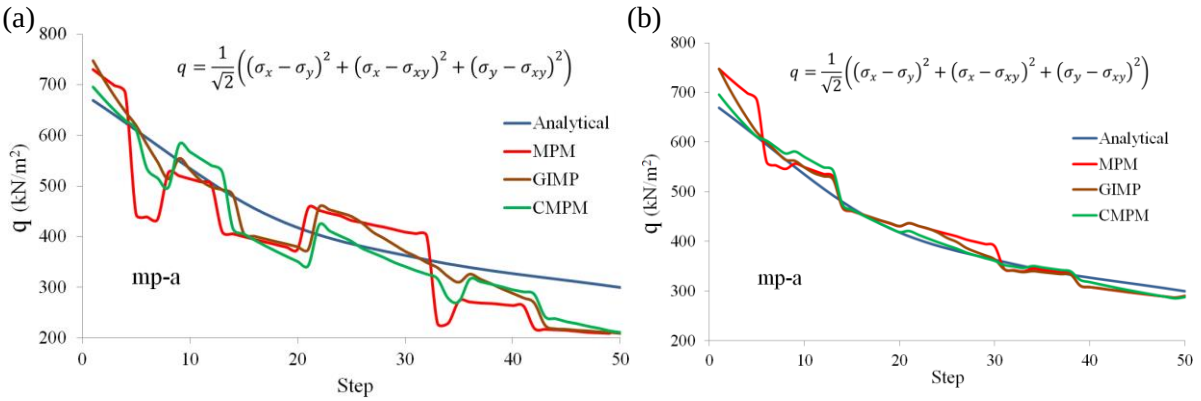

Fig. 5. mp-a deviatoric stress using (a) regular stiffness matrix, and (b) modified stiffness matrix.

4. Geotechnical application

To demonstrate the use of MPM, GIMP and CMPM in geotechnical problems, a vertical cutting stability problem has been analyzed, using a Von Mises constitutive model incorporating post-peak softening as described in [13]. Fig. 6 shows the initial geometry of the problem, characterized by a height of 1 m and a width of 2 m. The material is an elasto-plastic strain-softening soil, with elastic parameters E = 400 kPa and ν = 0.35. The peak and residual cohesions are 6 kPa and 1 kPa respectively, and the softening modulus is -25 kPa. In the domain, the left vertical boundary is fixed to prevent material point displacement in the horizontal direction, and the bottom boundary is fixed to prevent material point displacement in the vertical direction. The slope is loaded by gravity and the failure occurs due to its self weight. An explicit form of the code is used to solve the problem.

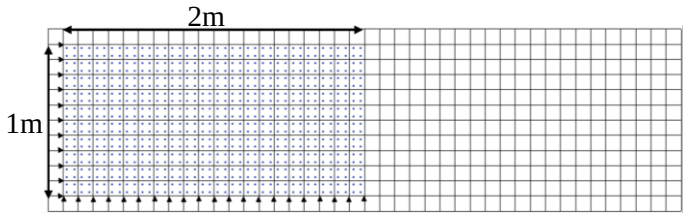

Fig. 6. Sketch of the initial material point locations and background mesh.

4.1 Results

The results after 10 cm of horizontal displacement at the toe are shown in Fig. 7. As can be seen, the stresses oscillate the most when using MPM, whereas GIMP and CMPM show a smoother development of the stresses and plastic strains around the developing band. During the earlier steps in the analysis, CMPM shows the smoothest results, but, since regular FE shape functions are used to perform the numerical integration, the CMPM accuracy decreases after several mesh crossings occur. Nevertheless, CMPM results are better than MPM because the imbalance caused by element crossing is attenuated by the use of non-local support (i.e. nodes outside the element). After large deformation, GIMP exhibits the smoothest results since the stresses are continuous. The plastic deformations shown are consistent between GIMP and CMPM, but more diffuse with MPM.

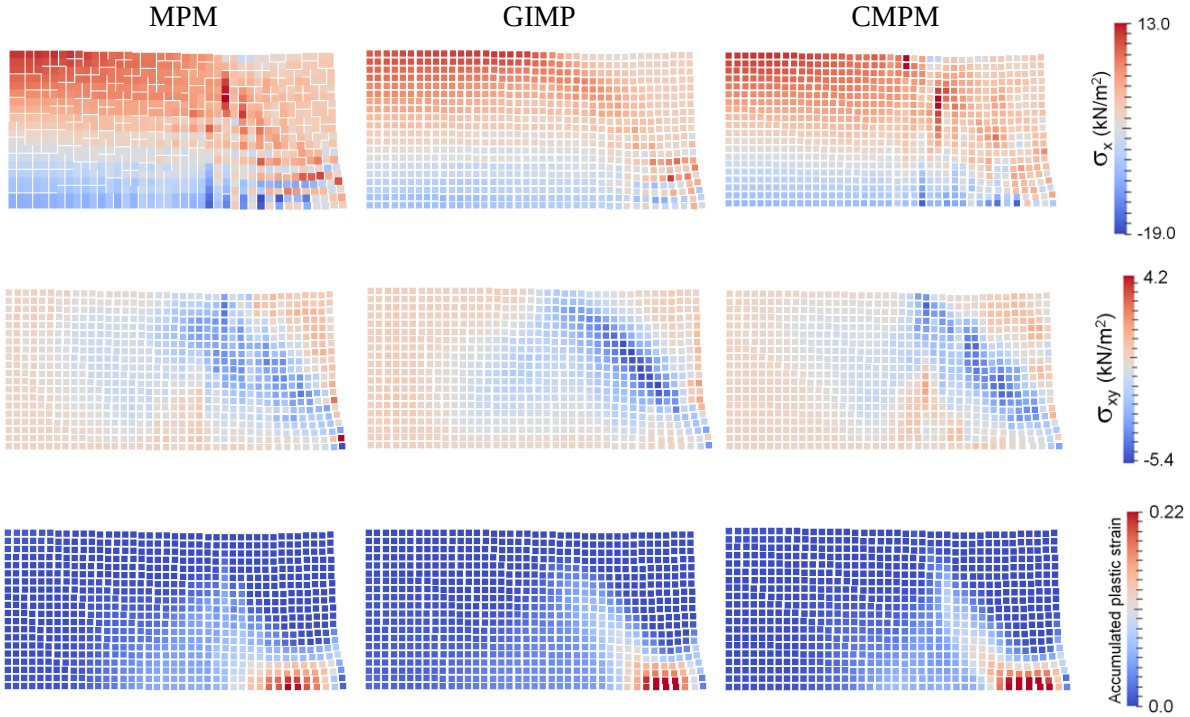

Fig. 7. Horizontal stress, shear stress and accumulated plastic strain contours with MPM, GIMP and CMPM.

5. Conclusions

This paper has investigated the imbalance caused by the use of regular FE shape functions to solve the governing equation in MPM, leading to the well-known stress oscillation problem. The use of CMPM and GIMP improves the accuracy of the results, since C^1, derivative continuous, shape functions are used to interpolate material point strains, reducing the oscillation caused by quadrature rule errors and element-crossing issues. It has been shown that CMPM can be used in implicit and explicit codes, and is able to compute more accurate stresses than MPM and GIMP. However, the accuracy of CMPM is only higher than GIMP until a certain point. This is because CMPM uses regular FE shape functions to compute internal and external loads, and this leads to oscillations when element crossing occurs. At this point, GIMP offers better results.

The additional oscillations caused by the stiffness matrix integration in implicit codes was also demonstrated. Since the stiffness of an element is governed by the number of material points within an element and the material point weighting value, during element crossing an irregular stiffness distribution over the domain is obtained, causing jumps in stresses. It has been shown that this problem can be reduced by the use of a modified weighting value that is a function of the initial element volume and the sum of the material point volumes inside the current element, leading to a smoother stiffness distribution.

References

[1] Sulsky D, Chen A, Schreyer HL. A particle method for history dependent materials. Comput. Methods Appl. Mech. Engng. 1994; 118: 179–196.
[2] Sulsky D, Zhou S, Schreyer HL. Application of a particle-in-cell method to solid mechanics. Computer Physics Communications. 1995; 87: 236–252.
[3] Bardenhagen S, Kober E. The generalized interpolation material point method. CMES: Comput. Model. Eng. Sci. 2004; 5: 447–495.
[4] Gonzalez Acosta L, Vardon PJ, Hicks MA. Compound material point method (CMPM) to improve stress recovery for quasi-static problems. Procedia Eng. 2017; 175: 324–331.
[5] Chen ZP, Qiu XM, Zhang X, Lian YP. Improved coupling of finite element method with material point method based on a particle-to-surface contact algorithm. Comput. Methods Appl. Mech. Engng. 2015; 293: 1–19.
[6] Wang B, Vardon PJ, Hicks MA. Investigation of retrogressive and progressive slope failure mechanisms using the material point method. Comput. Geotech. 2016; 78: 88–98.
[7] Wang B. Slope failure analysis using the material point method. PhD thesis, Delft University of Technology, 2016.
[8] Bathe KJ. Finite element procedures. Prentice Hall, New Jersey, 1982.
[9] Steffen M, Wallstedt PC, Guilkey JE, Kirby RM, Berzins M. Examination and analysis of implementation choices within the material point method (MPM). Comput. Model. Eng. Sci. 2008; 31: 107–127.
[10] Steffen M, Kirby RM, Berzins M. Analysis and reduction of quadrature errors in the material point method (MPM). Int. J. Numer. Meth. Engng. 2008; 76: 922–948.
[11] Zhang X, Chen Z, Liu Y. The material point method. A continuum-based particle method for extreme loading cases. Academic Press, 2016.
[12] Sadeghirad A, Astaneh AV. A finite element method with composite shape functions. Engineering Computations: Int. J. Computer-Aided Engng. Software. 2011; 28: 389–422.
[13] Wang B, Vardon PJ, Hicks MA. Development of an implicit material point method for geotechnical applications. Comput. Geotech. 2016; 71: 159–167.